

*\*\*A New Era in Cosmology\*\*  
 ASP Conference Series, Vol. **\*\*VOLUME\*\***, **\*\*PUBLICATION YEAR\*\***  
 \*\*Tom Shanks & Nigel Metcalfe, eds\*\**

## Studying the LSS through weak gravitational lensing maps

Antonio C. C. Guimarães

*Department of Physics, Brown University, Providence, RI 02912, USA*

**Abstract.** Weak gravitational lensing is a promising tool for the study of the mass distribution in the Universe. Here we report some partial results<sup>1</sup> that show how lensing maps can be used to differentiate between cosmological models. We pay special attention to the role of noise and smoothing. As an application, we use mock convergence fields constructed from N-body simulations of the large-scale structure for three historically important cosmological models. Various map analyses are used, including Minkowski functionals, and their ability to differentiate the models is calculated and discussed.

The images of distant galaxies are tangentially stretched in relation to mass concentrations in its light path. This weak gravitational lensing effect can be statistically measured and enables the construction of “lensing maps” (see Bartelmann & Schneider 2001 for a review of weak gravitational lensing). Here we focus on the convergence field  $\kappa$ , which can be calculated using

$$\kappa(\vec{\theta}) = \frac{3H_0^2}{2}\Omega_m \int_0^z g(z', z) \frac{\delta(\vec{\theta}, z')}{a(z')} dz' , \quad (1)$$

where  $\vec{\theta}$  is the angular position at the map,  $g$  a geometrical weighting factor,  $\delta$  the density contrast, and  $a$  the scale factor. This map contains information about the large-scale structure of the Universe (LSS). Our aim is to relate the characteristics of the convergence field to the LSS (see Jain, Seljak, & White 2000), and to discuss the ability of analyses of the convergence to differentiate between cosmological models. Our approach is to simulate  $\kappa(\vec{\theta})$  and use various statistics to characterize it.

We used N-body simulations (Hydra code - Couchman, Thomas, & Pearce 1995 - with  $128^3$  cold dark matter particles in boxes of side  $128h^{-1}Mpc$ ) to create realizations of the LSS between  $z = 0$  and a source redshift  $z = 1$ . A multiple-plane lens approximation to equation (1) was then used to generate 25 realizations of the convergence field. We considered three models: SCDM ( $\Omega_m = 1, \sigma_8 = 0.56$ ),  $\Lambda$ CDM ( $\Omega_m = 0.3, \Omega_\Lambda = 0.7, \sigma_8 = 0.99$ ), and OCDM ( $\Omega_m = 0.3, \Omega_\Lambda = 0, \sigma_8 = 0.84$ ). The indicated  $\sigma_8$  represents a normalization to the cluster abundance, and we adopt  $h = 0.7$ .

The generated fields had a minimum size of 9.6 degrees<sup>2</sup>, in a  $1024^2$  grid. We used a top-hat window of radius  $\theta_s$  to smooth the convergence field, and quantified it by calculating statistical measures. These included the convergence

---

<sup>1</sup>More complete and detailed results will be published elsewhere

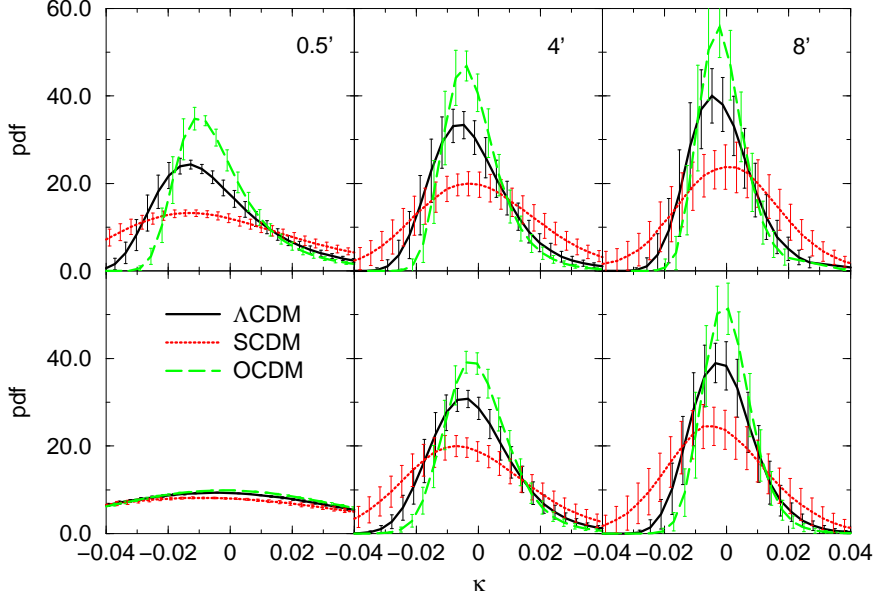


Figure 1. Probability distribution function of the convergence  $\kappa$  for  $\Lambda$ CDM (solid line), SCDM (dotted line), and OCDM (dashed line). Upper panels are for the pure field, and bottom panels for the noisy field. Three smoothing scales  $\theta_s$  are shown: 0.5 arcmin (left panels), 4 arcmin (central panels), and 8 arcmin (right panels).

field probability distribution function (PDF), root mean square ( $\sigma_\kappa^2 = \langle \kappa^2 \rangle$ ), skewness ( $S_3 = \langle \kappa^3 \rangle / \sigma_\kappa^4$ ), angular power spectrum ( $P_\kappa(l) = \langle |\tilde{\kappa}(l)|^2 \rangle$ ), and Minkowski functionals. Noise was included as a random Gaussian field with variance  $\sigma_n^2 = \sigma_\epsilon^2 / 2n_g \pi \theta_s^2$  ( $\sigma_\epsilon^2 = 0.16$  was the used value for the intrinsic ellipticity variance, and  $n_g = 60 \text{ arcmin}^{-2}$  the mean galaxy density), which was added to the pure convergence field (Van Waerbeke 2000).

We propose a method to quantitatively evaluate the ability of an analysis to differentiate between two weak lensing maps. Be  $A$  and  $B$  two lensing maps, and  $Y$  a vector-valued analysis.  $Y_A$  and  $Y_B$  are the result of applying the analysis  $Y$  on the maps  $A$  and  $B$ .  $Y_{A,B}$  is assumed to follow a normal distribution of mean value  $\bar{Y}_{A,B}$  and variance  $\sigma_{A,B}^2$ . We define the **differentiation** of the two maps under the analysis  $Y(p)$  ( $p$  labels the vector element) as

$$\mathcal{D}_Y(A, B) = 1 - e^{-\chi^2/2}, \quad (2)$$

where  $\chi^2 \equiv \sum_i [\bar{Y}_A(p_i) - \bar{Y}_B(p_i)]^2 / [\sigma_A^2(p_i) + \sigma_B^2(p_i)]$ .

The differentiation assumes a value close to zero when the maps are similar under the considered analysis, and close to one when the maps are very different. That enables one to quantitatively compare different analyses when these are applied to the same two maps.

Figure 1 shows the PDF results for the three considered models, which are compatible with the results of Munshi & Jain (2000). It illustrates the effect of smoothing and noise on the PDF analysis of the convergence field. Smoothing has the effect of reducing the root mean square (rms), or equivalently,

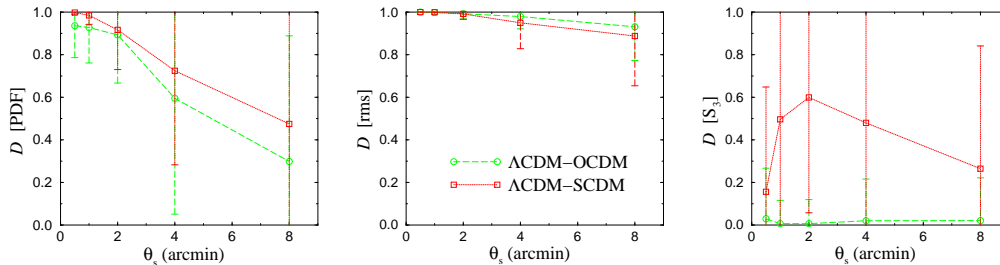


Figure 2. Differentiation between  $\Lambda$ CDM and SCDM (dotted line), and  $\Lambda$ CDM and OCDM (dashed line) for the analyses of the *noisy* convergence map, PDF (left panel), rms (central panel), and  $S_3$  (right panel).

the variance, and skewness of  $\kappa(\vec{\theta})$ . The addition of a noise field  $n(\vec{\theta})$  produces a PDF that can be described by the convolution of the pure convergence PDF  $F_{\kappa_o}$  with the noise PDF  $F_n$ ,

$$F_{\kappa}(x) = \int_{-\infty}^{+\infty} F_{\kappa_o}(y)F_n(x - y)dy, \quad (3)$$

the variance increases by the noise field variance ( $\sigma_{\kappa}^2 = \sigma_{\kappa_o}^2 + \sigma_n^2$ ), and the skewness is reduced by a factor,  $S_3(\kappa) = S_3(\kappa_o)(\sigma_{\kappa_o}/\sigma_{\kappa})^4$ .

The curves for the differentiation  $\mathcal{D}$  between the models are show in Figure 2. As expected, the smoothing of the field tends to make the models indistinct (decreasing  $\mathcal{D}$ ). Both the PDF and the simple rms analyses are able to distinguish the models at a significant confidence level at low smoothing. However, the skewness proves to be a bad analysis for differentiating these models (for convergence maps of the considered size and noise level), because the obtained  $\mathcal{D}_{S_3}$  is close to zero between  $\Lambda$ CDM and OCDM, and also because it is not very significant between  $\Lambda$ CDM and SCDM.

The addition of noise adds a power law to the power amplitude ( $P_{\kappa} = P_{\kappa_o} + P_n$ ). For small smoothing angular scales this contribution is significant, but it becomes negligible for large smoothing angular scales. However, at large smoothing angles power on small scales (large wavenumber  $l$ ) is suppressed - structure is washed out by the field smoothing (figure not shown).

The use of Minkowski functionals to characterize the morphology of the convergence field is another way to study the non-Gaussianity of  $\kappa$  (see Winitzki & Kosowsky 1998, Matsubara & Jain 2001, and Sato et al. 2001). Figure 3 shows some results for the Minkowski functionals analysis of  $\kappa$ ; the threshold  $\nu \equiv \kappa/\sigma_{\kappa}$  defines a 2D contour map, and the Minkowski functionals can be roughly described as the fractional area inside the contours ( $\nu_0$ ), the boundary length ( $\nu_1$ ), and the Euler characteristic ( $\nu_2$ ). Our results reveal that Minkowski functionals are very sensitive to noise and smoothing. The second functional ( $\nu_1$ ) have equal or even more discriminating power than the third functional ( $\nu_2$ ), and comparing their differentiation curves with the one for skewness, which also reflects non-Gaussian aspects of the convergence, their ability to discriminate between the considered models is superior. This differentiation is maximum for a median smoothing. At too small smoothing scales noise dominates, and at too large smoothing scales distinguishing features are erased.

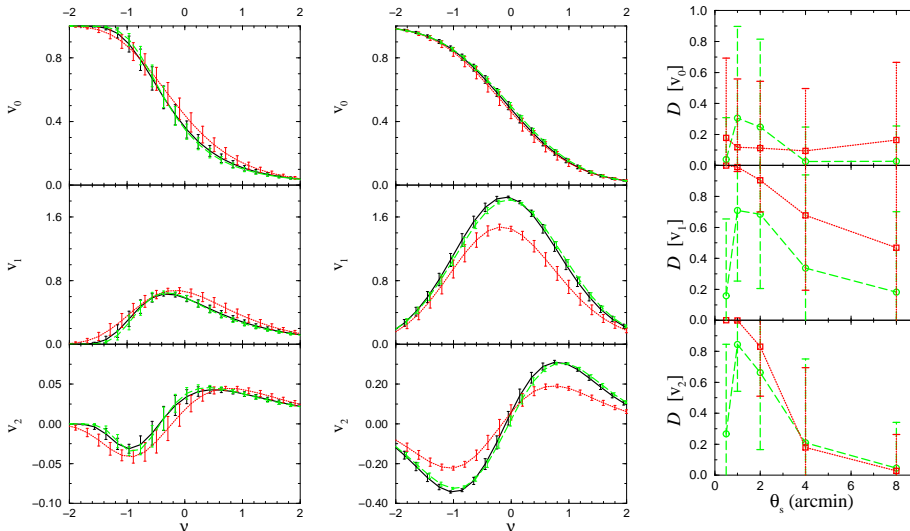


Figure 3. Minkowski functionals for the convergence field (pure at the left panel, and noisy at the central panel), for the three cosmological models considered (see Fig. 1), with  $\theta_s = 0.5$  arcmin smoothing. The right panel shows the differentiation between two models (see Fig. 2) under the Minkowski functionals analysis (noise included).

Our results indicate that a comprehensive study of the LSS through weak gravitational lensing maps requires the use of a set of analyses, because different analyses reveal distinct features of the underlying cosmic mass distribution and geometry. Also, the proposed quantity  $\mathcal{D}$  proved to be very useful for quantifying the differentiation between analyses of lensing maps, and for comparing different statistical measures of lensing.

**Acknowledgments.** ACCG thanks Uroš Seljak for providing codes and valuable knowhow, the Princeton University Physics Department for the use of its computer facilities, and also Robert H. Brandenberger and Ian dell’Antonio for very helpful discussions. The research at Brown was supported in part by the US Department of Energy under Contract DE-FG0291ER40688, Task A.

## References

- Bartelmann, M., & Schneider, P. 2001, *Phys.Rep.*, 340, 291  
 Couchman, H.M.P., Thomas, P.A., & Pearce, F.R. 1995, *ApJ*, 452, 797  
 Jain, B., Seljak, U., & White, S. 2000, *ApJ*, 530, 547  
 Munshi, D., & Jain, B. 2000, *MNRAS*, 318, 109  
 Matsubara, T., & Jain, B. 2001, *ApJ*, 552, L89  
 Sato, J., Takada, M., Jing, Y.P., & Futamase, T. 2001, *ApJ*, 551, L5  
 Van Waerbeke, L. 2000, *MNRAS*, 313, 524  
 Winitzki, S., & Kosowsky, A. 1998, *New Astron.*, 3, 75